Generator dynamics in aeroelastic analysis and simulations

Larsen, Torben J.; Hansen, Morten Hartvig; Iov, F.

Publication date:
2003

Document Version
Publisher's PDF, also known as Version of record

Risø-R-1395(EN)

Generator Dynamics in Aeroelastic Analysis and Simulations

Torben J. Larsen, Morten Hartvig Hansen, Florin Iov

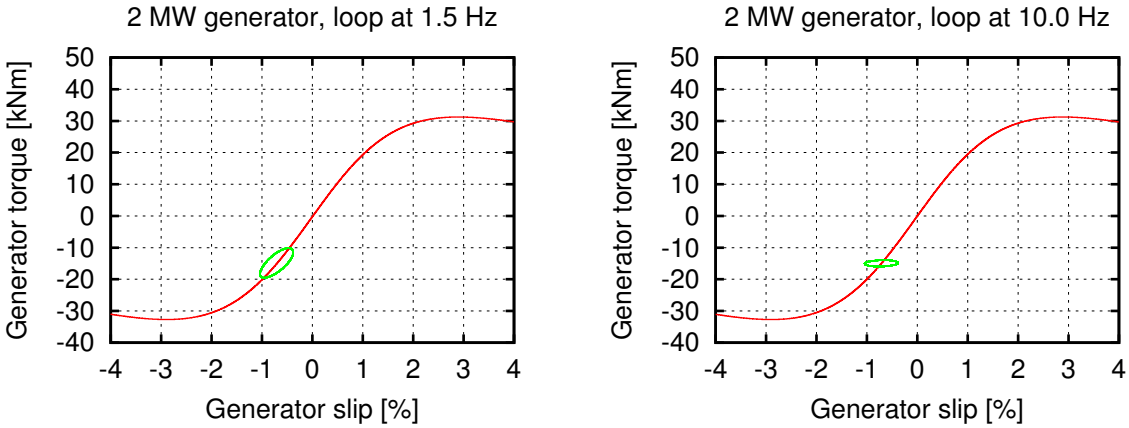

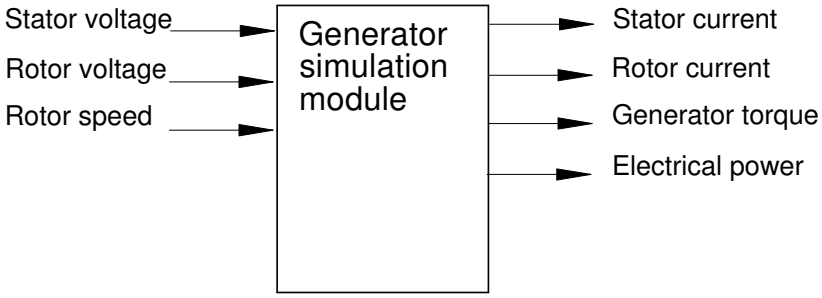

Risø National Laboratory, Roskilde, Denmark
July 2003

Abstract This report contains a description of a dynamic model for a doubly-fed induction generator implemented in the aeroelastic code HAWC. The model has physical input parameters (resistance, reactance etc.) and input variables (stator and rotor voltage and rotor speed). The model can be used to simulate the generator torque as well as the rotor and stator currents, active and reactive power.

A perturbation method has been used to reduce the original generator model equations to a set of equations which can be solved with the same time steps as a typical aeroelastic code. The method is used to separate the fast transients of the model from the slow variations and deduce a reduced order expression for the slow part.

Dynamic effects of the first order terms in the model as well as the influence on drive train eigenfrequencies and damping has been investigated. Load response during time simulation of wind turbine response have been compared to simulations with a linear static generator model originally implemented i HAWC.

A 2 MW turbine has been modelled in the aeroelastic code HAWC. When using the new dynamic generator model there is an interesting coupling between the generator dynamics and a global turbine vibration mode at 4.5 Hz, which only occurs when a dynamic formulation of the generator equations is applied. This frequency can especially be seen in the electrical power of the generator and the rotational speed of the generator, but also as torque variations in the drive train.

The present report has passed an internal review at the Wind Energy Department at Risø National Laboratory, performed by:

Kenneth Thomsen *Poul Sørensen* *Anca Hansen*

ISBN 87-550-3188-9
ISBN 87-550-3189-7 (internet)
ISSN 0106-2840

Print: Pitney Bowes Management Services Denmark A/S, 2003.

Contents

Acknowledgements

This report presents the work and results carried out during the national projects "Simulation platform for modelling, optimization and design of wind turbines EFP-1363/01-0013" and "Application, demonstration and further development of advanced aerodynamic and aeroelastic models ENS-1363/02-0011" both funded by the Danish Energy Agency, and the international project "Aeroelastic Stability and Control of Large Wind Turbines NNE5-CT-2002-00627" partly funded by the European Commision.

1 Introduction

The fact that wind turbines have grown in size and thereby become a more important supplier to the electrical grid, more focus has been on the quality of the electrical power during the last years. The demand of a wind turbine to be able to maximize power output yet minimize consumption of reactive power and even to control the reactive power, is becoming more important. This, together with the fact that generator dynamics is important to the drive train dynamics, makes it important that the wind turbine simulation tools, that are allready developed, also includes physical models of generators.

This report describes a physical nonlinear dynamic model with only few limitations, see Section 2, and in particular a case study of the influence in aeroelastic simulations of a wind turbine with this model implemented compared to the use of generator models traditionally used in aeroelastic codes. The generator model described in this report can be used both for a doubly-fed induction generator and for an asynchronous generator where the rotor is short circuit. The investigations done in this report only covers the asynchronous application.

The traditional generator models used in aeroelastic codes have so far been rather simple static models providing a linear relationship between the generator speed and torque based on generator slip, which is a simplified implementation of a classic steady-state model. Regarding the classic steady-state way of modelling generator torque-speed relation, the dynamic performance of the induction machines is not predicted accurately as reported in [1], [2] and [3]. In the last years some new approaches in the reduced order modelling of the induction machine are reported in the litterature. A simplified second-order model (two degrees of freedom) has been developed as an alternative to a third-order in [4] and [5]. Reduced order models have been obtained for synchronous generators based on integral manifolds theory in [6] and [7], and extended to induction machines in [2] and [3].

The starting point of the work in this report is a full nonlinear dynamic model of an induction generator described by Kovacs [8]. Since the equations for this model needs a solution sample frequency very high compared to normal aeroelastic calculations, a reduced order model has been used that only includes the low frequent part of the transients, i.e. only the dynamics of the rotor. To verify the reduced dynamic model a perturbation method has been used. Using this method the original generator model expressions have been separated in fast and slow variation components. The slow variation components corresponds to the equations that can be deduced from the original generator equations when neglecting the transients of the stator flux.

Dynamic effects of the first order terms in the model as well as the influence on drive train eigenfrequencies and damping has been investigated for an asynchronous generator. Load response during time simulation of wind turbine response has been compared the response using simulations with a traditional static linearised generator model.

For the 2 MW turbine modelled, there is an interesting coupling between the generator dynamics and a global turbine vibration mode at 4.5 Hz, which only occurs when a dynamic formulation of the generator equations is applied.

2 Generator formulation

The dynamic equations of the rotor and stator of the generator can be formulated in a d-q synchronous reference frame that mean a reference frame rotating with the stator voltage. The equations are thereby formulated in complex form where the real part is the axis following the reference frame and the imaginary part is with a phase shift of 90 degrees, see Figure 1.

2.1 Symbol list

Symbol	Description
f_{net}	Grid frequency
i_s	Current in stator, $i_s = i_{sd} + ji_{sq}$
i_r	Current in rotor, $i_r = i_{rd} + ji_{rq}$
j	complex operator, $j = \sqrt{-1}$
p	pole pairs
S_r	Apparent power of rotor, $S_r = P_r + jQ_r$
S_s	Apparent power of stator, $S_s = P_s + jQ_s$
R_s	Stator resistance
R_r	Rotor resistance
s	Generator slip
T	Generator torque
u_r	Voltage rotor, $u_r = u_{rd} + ju_{rq}$
u_s	Voltage stator, $u_s = u_{sd} + ju_{sq}$
ω_e	Synchronous speed, $\omega_e = 2\pi f_{net}$
ω_r	Electrical rotor speed, $\omega_r = p\Omega_r$
Ω_r	Mechanical rotor speed
P_r	Active power of rotor
P_s	Active power of stator
Q_r	Reactive power of rotor
Q_s	Reactive power of stator
X_m	Magnetizing reactance
X_r	Rotor leakage reactance
X_s	Stator leakage reactance
ψ_r	Flux, rotor ($\psi_r = \psi_{rd} + j\psi_{rq}$)
ψ_s	Flux, stator ($\psi_s = \psi_{sd} + j\psi_{sq}$)

Table 1. Describtion of symbols used in the report

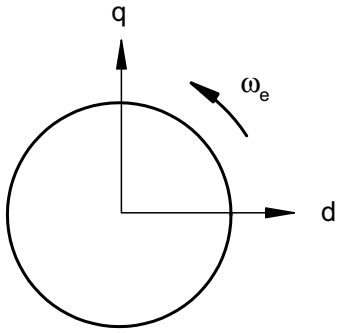

Figure 1. d-q coordinate system related to grid rotation direction. d represents real part and q the imaginary part of complex notations in this report.

2.2 Full dynamic model

The voltage equations for the induction machine in a d-q synchronous reference frame, see Figure 1, can be written in complex form with the real axis d and the imaginary axis q according to [8]:

$$\begin{aligned} u_s &= R_s i_s + \dot{\psi}_s + j\omega_e \psi_s \\ u_r &= R_r i_r + \dot{\psi}_r + j\left(\omega_e - \omega_r\right)\psi_r \end{aligned} \tag{1}$$

where $\dot{\psi}$ denotes $\frac{d\psi}{dt}$ and $j = \sqrt{-1}$.

The relation between current i and flux ψ is according to [8] given

$$\left\{ \begin{array}{c} \psi_s \\ \psi_r \end{array} \right\} = \left[\begin{array}{cc} L_{ss} & L_m \\ L_m & L_{rr} \end{array} \right] \left\{ \begin{array}{c} i_s \\ i_r \end{array} \right\} \tag{2}$$

where

$$\begin{aligned} L_m &= \frac{X_m}{\omega_e} \\ L_{ss} &= \frac{X_m + X_s}{\omega_e} \\ L_{rr} &= \frac{X_m + X_r}{\omega_e} \end{aligned} \tag{3}$$

(2) is written in a more convenient way as

$$\left\{ \begin{array}{c} i_s \\ i_r \end{array} \right\} = \frac{1}{D} \left[\begin{array}{cc} L_{rr} & -L_m \\ -L_m & L_{ss} \end{array} \right] \left\{ \begin{array}{c} \psi_s \\ \psi_r \end{array} \right\} \tag{4}$$

where $D = L_{ss}L_{rr} - L_m^2$

By inserting the expression of current in (4) into (1) the behaviour of the generator based on electro-magnetic fluxes in (5) is obtained.

$$\left\{ \begin{array}{c} \dot{\psi}_s \\ \dot{\psi}_r \end{array} \right\} = \left[\begin{array}{cc} -\frac{R_s L_{rr}}{D} - j\omega_e & \frac{R_s L_m}{D} \\ \frac{R_r L_m}{D} & -\frac{R_r L_{ss}}{D} - j\left(\omega_e - \omega_r\right) \end{array} \right] \left\{ \begin{array}{c} \psi_s \\ \psi_r \end{array} \right\} + \left\{ \begin{array}{c} u_s \\ u_r \end{array} \right\} \quad (5)$$

The electrical power on stator and rotor respectively is calculated from the voltage and current of the generator.

$$\begin{aligned} S_s &= \frac{3}{2} u_s \bar{i}_s \\ S_r &= \frac{3}{2} u_r \bar{i}_r \end{aligned} \quad (6)$$

where $\bar{i}$ denotes the complex conjugate of i. The real part of the power is the active power P and the imaginary part is the reactive power Q.

The electromagnetic torque of the generator is according to [8] calculated as

$$T = \frac{3}{2} \mathrm{Im}\{\bar{\psi}_s i_s\} \quad (7)$$

In eqrefeq:torque-kovacs it was assumed that the number of pole pairs $p = 1$. With more pairs, the number has to be taken into account which increase the torque in (7) with a factor of p. The torque can therefore be expressed based entirely on fluxes as in (8).

$$T = \frac{3pL_m}{2D} \mathrm{Im}\{\psi_s \bar{\psi}_r\} \quad (8)$$

2.3 Reduced dynamic model

The equations in (5) must be solved with a very small time step $\approx$ 1-2 ms to avoid numerical instability, when using a standard Runge-Kutta solver. This is very unfortunately related to aeroelastic simulations since only frequencies up to 10-15 Hz are important for the structural behavior regarding load response. The sample frequency in a structural solver is therefore normally in the size of 50 Hz. To eliminate the need for very small sample steps the equation (5) is modified. We assume that the stator flux is almost constant ($\dot{\psi_s} \equiv 0$), which is often used to reduce the order of induction generator models e.g. for wind turbine simulations in [9] and mathematical justified in Section 3.

By assuming $\dot{\psi_s} \equiv 0$, equation (5) is rewritten to one complex differential equation describing the rotor flux

$$\dot{\psi_r} = \left(\frac{R_r R_s L_m^2}{D^2 \left(\frac{R_s L_{rr}}{D} + j\omega_e \right)} - \frac{R_r L_{ss}}{D} - j\left(\omega_e - \omega_r\right) \right) \psi_r + \frac{R_r L_m}{D \left(\frac{R s L_{rr}}{D} + j\omega_e \right)} u_s + u_r \tag{9}$$

and one complex equation describing the stator flux

$$\psi_s = \frac{R_s L_m}{D \left(\frac{R s L_{rr}}{D} + j\omega_e \right)} \psi_r + \frac{u_s}{\frac{R_s L_{rr}}{D} + j\omega_e} \tag{10}$$

The solution of (9) and (10) can be performed at every time step of a simulation using eg. the Runge-Kutta method on (9) and solving (10) with the result of (9) with a sample frequency down to $\sim$ 40 Hz.

To illustrate the behavior of the reduced dynamic model compared to the full dynamic model some test simulations have been done. In Figure 2 is illustrated a cut-in simulation with both the full dynamic model and the reduced dynamic model. In the cut-in situation no soft starter has been included, hence large transient occurs. The full dynamic model has been performed with a sample frequency of 1000 Hz whereas the reduced dynamic model has been performed with a sample frequency of 50 Hz. It is seen that the difference in the results of the two models is the fast (50 Hz) transient on the electrical side. The mechanical generator shaft torque is not affected by this fast fluctuation at all, hence the reduced dynamic model is suitable for structural calculations.

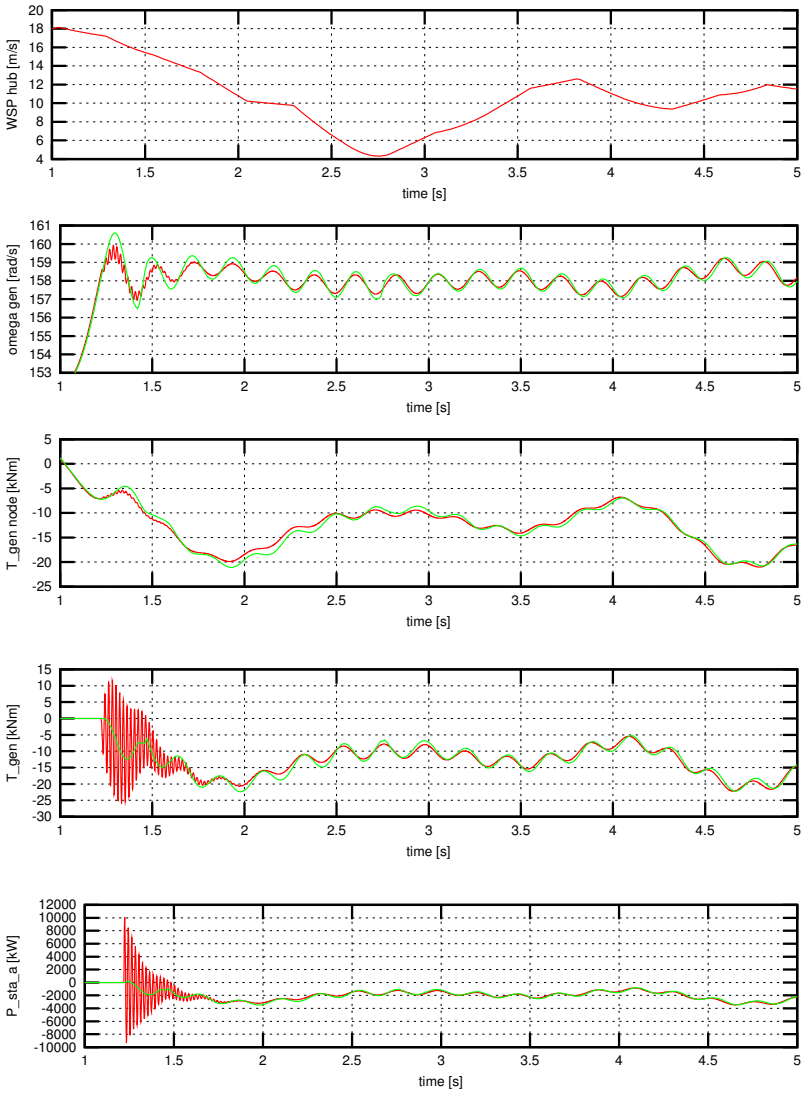

Figure 2. Comparison of full dynamic model with reduced dynamic model at cut-in situation without soft starter. From top: Wind speed at hub [m/s], rotational speed generator [rad/s], structural generator torque [kNm], electro-mechanical generator torque [kNm], electrical power stator (active) [kW].

3 Perturbation analysis

The purpose of this section is to justify the assumption of the quasi-steady conditions for the stator flux used in the reduced model, and to analyze the basic dynamics of induction machines.

A perturbation method known as *Direct Partition of Motion* (see e.g. [10, 11]) is used in Section 3.2 to show that the time-derivative in the stator equation (5) can be neglected when considering only *slow variations* in fluxes. Furthermore, it is shown that the *fast variations* in stator flux have no important effect on the low frequency response for small perturbations from a steady state equilibrium of the generator. This does not hold for abrupt changes of generator conditions.

A local analysis of the nonlinear generator dynamics is performed in Section 3.3 for a 2 MW machine. It is shown that both the reduced and full model predict a distinct natural frequency, which is of the same order as the natural frequencies of turbine structure. Hence, the dynamics of induction machines must be considered in aeroelastic computations of turbines.

3.1 Coupled equations of motion

The equations for the generator fluxes (5) are coupled with a dynamic slip equation describing equilibrium between electromagnetic torque (8), mechanical torque and the moment of inertia needed to accelerate the generator rotor:

$$J\,\dot{\Omega}_r = T + T_m \tag{11}$$

where $(\dot{}) \equiv \partial/\partial t$, T_m is the mechanical torque and J is the moment of inertia for the generator rotor including part of the high speed drive-train, especially the brake disc. The slip is defined as $s \equiv (\omega_e - p\,\Omega_r)/\omega_e$, where it is noted that the slip is negative ($s < 0$) for induction machines used as generators. Using this definition, the equilibrium of moments (11) can be written in terms of the slip as

$$\dot{s} + \frac{3}{2}\,\frac{p^2\,L_m}{J\,\omega_e\,D}\,\mathrm{Im}\Big\{\psi_s\,\overline{\psi}_r\Big\} = -\frac{p\,T_m}{J\,\omega_e} \tag{12}$$

which couples nonlinearily to the flux equations (5).

To perform the perturbation analysis of the coupled set of governing equations, the order of magnitude of the their terms must be weighted. This weighting is initiated by an introduction of the following non-dimensional parameters:

$$\begin{aligned}
\gamma_{sr} &= \frac{R_s L_{rr}}{\omega_e D} = \frac{R_s X_m + R_s X_r}{(X_s + X_r)X_m + X_s X_r} \\
\gamma_{rs} &= \frac{R_r L_{ss}}{\omega_e D} = \frac{R_r X_m + R_r X_s}{(X_s + X_r)X_m + X_s X_r} \\
\gamma_{sm} &= \frac{R_s L_m}{\omega_e D} = \frac{R_s X_m}{(X_s + X_r)X_m + X_s X_r} \\
\gamma_{rm} &= \frac{R_r L_m}{\omega_e D} = \frac{R_r X_m}{(X_s + X_r)X_m + X_s X_r}
\end{aligned} \tag{13}$$

All these parameters are small $\gamma_{sr}, \gamma_{rs}, \gamma_{sm}, \gamma_{rm} << 1$. This presumption can be justified by noting that the stator and rotor leakage reactances are an order of magnitude smaller than the magnetizing reactance ($X_s, X_r << X_m$), and that the stator and rotor resistances are an order of magnitude smaller than the sum of the stator and rotor leakage reactances ($R_s, R_r << X_s + X_r$), where the last assumption is not always true, but the error of the assumption is not severe. The error in the perturbation method increase as the assumptions correctness decrease.

A small book-keeping parameter $\epsilon << 1$ is introduced to denote small terms in the following perturbation analysis. The low order of magnitude of the non-dimensional parameters in (13) can be expressed by $\gamma_{\alpha\beta} = O(\epsilon)$, whereas the grid frequency has a large order of magnitude $\omega_e = O(\epsilon^{-1})$. For the voltages over stator and rotor it is known that $|u_r| << |u_s|$ for a doubly-fed generator, and $u_r = 0$ for generators with a short-circuited rotor. The magnitude of the stator voltage is of same order as the grid frequency $|u_s| = O(\epsilon^{-1})$. The slip is small $s = O(\epsilon)$, and the other terms in the slip equation are also assumed to be small $p^2 L_m/(J\omega_e D) = O(\epsilon)$ and $pT_a/(J\,\omega_e) = O(\epsilon)$.

Hence, the set of weighted governing equations are given by

$$\begin{aligned}
\dot{\psi}_s + \epsilon^{-1}\,\omega_e(\gamma_{sr} + j)\;\psi_s - \omega_e\gamma_{sm}\;\psi_r &= \epsilon^{-1}\,u_s \\
\dot{\psi}_r + \omega_e(\gamma_{rs} + j\,s)\;\psi_r - \omega_e\gamma_{rm}\;\psi_s &= u_r \\
\dot{s} + \frac{3}{2}\,\frac{p^2\,L_m}{J\,\omega_e\,D}\,\mathrm{Im}\Big\{\psi_s\,\overline{\psi}_r\Big\} &= -\frac{p\,T_m}{J\,\omega_e}
\end{aligned} \tag{14}$$

where two terms of the stator equation are large compared to the other terms, whereas all terms of the equations for rotor flux and slip are of the same order. The orders of the time derivatives are unknown for both fluxes and slip.

3.2 Separation of fast and slow variations

Direct Partition of Motion can be applied to dynamic systems with several time-scales. The system of coupled generator equations (14) is assumed to contain two distinct time-scales

$$T_0 = \omega_e t \qquad \text{and} \qquad T_1 = t \tag{15}$$

where the fast time-scale T_0 corresponds to the rate of the grid oscillations, and the slow time-scale T_1 corresponds to the rate of mechanical torque variations ($T_m = T_m(T_1)$) due to the aeroelastic behavior of the turbine.

A perturbation solution of the coupled equations is sought, where the variations of fluxes and slip can be separated into slow and fast parts

$$\begin{aligned}
\psi_s &= \psi_{s_0}(T_1) + \psi_{s_1}(T_0, T_1) \\
\psi_r &= \psi_{r_0}(T_1) + \epsilon\,\psi_{r_1}(T_0, T_1) \\
s &= s_0(T_1) + \epsilon\,s_1(T_0, T_1)
\end{aligned} \tag{16}$$

where the fast variations of rotor fluxes and slip are assumed to be small compared to the corresponding slow variations ($\psi_{r_1} << \psi_{r_0}$ and $s_1 << s_0$). The fast variation of stator flux is assumed to be of the same order as the slow variation, because transients in stator flux due to grid failure or cut-in, can be dominated by components at the grid frequency. The individual weighting of the fast and slow components of each state variable is not important for the derivation of the reduced model, i.e., the governing equations for variations on the slow time-scale.

The key to the separation of fast and slow variations are that the fast variations are presumed to have zero averages over one period of grid oscillation. A linear T_0-averaging operator is defined as

$$\langle\ \rangle \equiv \tfrac{1}{2\pi}\int_0^{2\pi}(\ )dT_0 \tag{17}$$

whereby this average conditions for the separation of motion can be written as

$$\langle\psi_s\rangle = \psi_{s_0}(T_1)\ , \qquad \langle\psi_r\rangle = \psi_{r_0}(T_1) \qquad \text{and} \qquad \langle s\rangle = s_0(T_1) \tag{18}$$

Note that the solution form (16) can be considered as a transformation of the average of the fluxes and the slip. Using that $\omega_e = O(\epsilon^{-1})$, the time-derivatives of the fluxes and the slip are written as

$$\begin{aligned}
\dot{\psi}_s &= \epsilon^{-1}\,\omega_e\,D_0\,\psi_{s_1} + D_1\psi_{s_0} + D_1\psi_{s_1} \\
\dot{\psi}_r &= \omega_e\,D_0\,\psi_{r_1} + D_1\psi_{r_0} + \epsilon\,D_1\psi_{r_1} \\
\dot{s} &= \omega_e D_0 s_1 + D_1 s_0 + \epsilon\,D_1 s_1
\end{aligned} \tag{19}$$

where $D_j \equiv \partial/\partial T_j$ are the derivatives with respect to the two time-scales.

To obtain the governing equations for the fast and slow variations, equations (16) and (19) are inserted into equations (14). The equation of slow variations is obtained by evaluating the T_0-average of the resulting equations:

$$\begin{aligned}
D_1\psi_{s_0} + \epsilon^{-1}\,\omega_e(\gamma_{sr}+j)\,\psi_{s_0} - \omega_e\gamma_{sm}\,\psi_{r_0} &= \epsilon^{-1}\,u_s \\
D_1\psi_{r_0} + \omega_e(\gamma_{rs}+j\,s_0)\,\psi_{r_0} + j\,\epsilon^2\,\omega_e\big\langle s_1\psi_{r_1}\big\rangle - \omega_e\gamma_{rm}\,\psi_{s_0} &= u_r \\
D_1 s_0 + \frac{3}{2}\,\frac{p^2\,L_m}{J\,\omega_e\,D}\,\mathrm{Im}\Big\{\psi_{s_0}\,\overline{\psi}_{r_0} + \epsilon\,\big\langle\psi_{s_1}\overline{\psi}_{r_1}\big\rangle\Big\} &= -\frac{p\,T_m}{J\,\omega_e}
\end{aligned} \tag{20}$$

where conditions (18) and that $\langle T_m\rangle = T_m(T_1)$ have been used. Subtraction of these T_0-averaged equations from the full equations yields the equations of fast variations

$$\begin{aligned}
\epsilon^{-1}\,\omega_e\,D_0\psi_{s_1} + D_1\psi_{s_1} + \epsilon^{-1}\,\omega_e(\gamma_{sr}+j)\psi_{s_1} - \epsilon\,\omega_e\gamma_{sm}\psi_{r_1} &= 0 \\
\omega_e D_0\psi_{r_1} + \epsilon D_1\psi_{r_1} + \epsilon\omega_e(\gamma_{rs}+j s_0)\psi_{r_1} + j\epsilon\omega_e\psi_{r_0}s_1 - \omega_e\gamma_{rm}\psi_{s_1} &= 0 \\
\omega_e\,D_0 s_1 + \epsilon\,D_1 s_1 + \frac{3}{2}\,\frac{p^2\,L_m}{J\,\omega_e\,D}\,\mathrm{Im}\Big\{\psi_{s_1}\,\overline{\psi}_{r_0} + \epsilon\,\psi_{s_0}\,\overline{\psi}_{r_1}\Big\} &= 0
\end{aligned} \tag{21}$$

It is noted that the equations of slow variations (20) are identical to the full equations (14) except that the dominating terms have now been determined. Evaluation of these terms of highest order yields an approximation to the slow variations of fluxes and slip due to slow variations of mechanical torque

$$\begin{aligned} \omega_e(\gamma_{sr}+j)\,\psi_{s_0} - \omega_e\gamma_{sm}\,\psi_{r_0} &= u_s \\ \dot{\psi}_{r_0} + \omega_e(\gamma_{rs}+j\,s)\,\psi_{r_0} - \omega_e\gamma_{rm}\,\psi_{s_0} &= u_r \\ \dot{s}_0 + \frac{3}{2}\,\frac{p^2\,L_m}{J\,\omega_e\,D}\,\mathrm{Im}\Big\{\psi_{s_0}\,\overline{\psi}_{r_0}\Big\} &= -\frac{p\,T_m}{J\,\omega_e} \end{aligned} \tag{22}$$

where the term $-\omega_e\gamma_{sm}\,\psi_{r_0}$ in the equation of slow stator flux variation (20) has been retained although it is an order lower than the dominating terms. It has not been determined from the perturbation analysis whether this term is larger than the time-derivative term. However, this term must be included in the stator equation of (22) to ensure that the steady state fluxes and torque modelled by the reduced model are the same as those modelled by the full model.

The equations of slow variations (22) contain no fast components, thus it is possible to separate the fast and slow variation under the assumption that the fast variations are sufficiently small. However, abrupt changes during a grid failure will lead to large fast variations in stator and rotor fluxes. These will have an important effect on the slow variations of rotor flux and slip through the terms $\langle s_1\overline{\psi}_{r_1}\rangle$ and $\langle\psi_{s_1}\overline{\psi}_{r_1}\rangle$, respectively (cf. equation (20)).

The dominating terms of the equations of fast variations (23) govern small fast transients that may occur in the fluxes and slip during a smooth cut-in sequence. Evaluation of these terms of highest order yields

$$\begin{aligned} D_0\psi_{s_1} + \omega_e(\gamma_{sr}+j)\psi_{s_1} &= 0 \\ \omega_e D_0\psi_{r_1} - \omega_e\gamma_{rm}\psi_{s_1} &= 0 \\ \omega_e\,D_0 s_1 + \frac{3}{2}\,\frac{p^2\,L_m}{J\,\omega_e\,D}\,\mathrm{Im}\Big\{\psi_{s_1}\,\overline{\psi}_{r_0}\Big\} &= 0 \end{aligned} \tag{23}$$

Assuming that the slow variation of rotor flux is constant $\psi_{r_0} = \psi_r^0$ in the fast time-scale T_0, the solutions of (23) become

$$\begin{aligned} \psi_{s_1} &= c_1 e^{-\gamma_{sr}\omega_e t} e^{-j\omega_e t} \\ \psi_{r_1} &= \frac{c_1}{\gamma_{sr}+j}\,e^{-\gamma_{sr}\omega_e t} e^{-j\omega_e t} + c_2 \\ s_1 &= -\frac{3}{2}\,\frac{p^2\,L_m}{J\,\omega_e^2\,D(\gamma_{sr}^2+1)} e^{-\gamma_{rs}\omega_e t}\Big(\,|c_1|\,|\psi_r^0|\,\cos(\omega_e t - \phi_s + \phi_r) \\ &\qquad -\gamma_{rs}\,|c_1|\,|\psi_r^0|\,\sin(\omega_e t - \phi_s + \phi_r)\Big) + c_3 \end{aligned} \tag{24}$$

where c_1, c_2 and c_3 are integration constants, and $\phi_r = \arg(\psi_r^0)$ and $\phi_s = \arg(c_1)$. The condition that the fast variations must have zero T_0-averages implies that $c_2 = c_3 = 0$. Thus, the fast transients are determined by a single complex constant c_1, which describes the perturbation of stator flux from its steady state value at the initial conditions.

3.3 Local analysis of generator dynamics

This section deals with a local analysis of generator dynamics including numerical examples based on the 2 MW turbine defined in Table 2 and the short-circuited generator defined in Table 3. Note that the moment of inertia of the generator rotor is listed as 65 kgm^2. Including added inertia from the adjacent mass such as the brake disc, the following examples have been computed with J=150 kgm^2.

First, the fluxes at the steady state equilibrium between electromagnetic and mechanical torque is derived as functions of the steady slip, which again is given implicit by the constant mechanical torque. Second, the transients response of the 2 MW machine during a special cut-in are computed based on the full and reduced models to show a good agreement. These transients are shown to have a distinct low frequency component, corresponding to a natural frequency computed at the end of the section, see Figure 4.

Steady state

The mechanical torque is assumed to be constant, hence there exists a steady state equilibrium for the full set of equations (14) and the reduced set of equations (22). Insertion of the steady solution ($\psi_s = \psi_s^0$, $\psi_r = \psi_r^0$, $s = s^0$) into either one of these two coupled equations, the following implicit solution can be found:

$$\begin{aligned} \psi_s^0 &= \frac{u_s(\gamma_{rs} + js^0) + \gamma_{sm} u_r}{\omega_e((\gamma_{sr} + j)(\gamma_{rs} + js^0) - \gamma_{rm}\gamma_{sm})} \\ \psi_r^0 &= \frac{\gamma_{rm} u_s + (\gamma_{sr} + j) u_r}{\omega_e((\gamma_{sr} + j)(\gamma_{rs} + js^0) - \gamma_{rm}\gamma_{sm})} \\ T_0 &= \frac{3}{2}\frac{p\,L_m}{D}\,\mathrm{Im}\Big\{\psi_s^0\,\overline{\psi}_r^0\Big\} = -T_m \end{aligned} \tag{25}$$

where the steady slip s^0 can be determined by solving the nonlinear equation $T_0(s^0) = -T_m$, stating that the steady electromagnetic torque must balance the constant mechanical torque. The steady torque T_0 has extrema at the pull-out slip s_p defined as

$$\left.\frac{dT_0}{ds^0}\right|_{s^0=s_p} = 0 \tag{26}$$

and the corresponding pull-out torque is $T_p = T_0(s_p)$.

For a short-circuited machine ($u_r = 0$) the pull-out slip depends only on the non-dimensional parameters given by (13), whereas the pull-out slip for a doubly-fed machine depends additionally on the voltages over the stator and rotor. Using that the non-dimensional parameters given by (13) are all small, the pull-out slip and torque of a short-circuited generator can be approximated by

$$s_p \approx -\gamma_{rs} \qquad \text{and} \qquad T_p \approx -\frac{3}{4}\frac{p\,L_m}{D}\frac{\gamma_{rm}}{\gamma_{rs}}\frac{u_{sd}}{\omega_e^2} \tag{27}$$

where u_{s_d} is the constant (real) stator voltage. The slope of the steady torque at zero slip can be approximated by

$$\left.\frac{dT_0}{ds_0}\right|_{s_0=0} \approx \frac{3}{2}\,\frac{p\,L_m}{D}\,\frac{\gamma_{rm}}{\gamma_{rs}^2}\,\frac{u_{sd}}{\omega_e^2} = \frac{2\,T_p}{s_p} \tag{28}$$

These results for short-circuited machines can also be found in [8] for the case of a single pole pair ($p = 1$).

Figure 3 shows an example of the steady torque as function of slip for the short-circuited 2 MW induction machine defined in Table 2 and 3. The pull-out slip is 2.90 % and the pull-out torque is 32.75 kNm computed by equation (27). The approximate relation between slope at zero slip with these pull-out values given by (28) is indicated by the dashed lines.

Transient response

The transient responses described by the full model (14) and reduced model (22) are computed to validate the perturbation solution and the assumption of neglecting the time-derivative in the stator equation leading to the reduced model.

The time simulations are initiated at a theoretical cut-in point, where the slip has reached its steady state value, but the fluxes only have reached 90 % of their steady state values given by (25) for the steady slip. The initial conditions for the simulation are therefore

$$\psi_s(0) = 0.9\;\psi_s^0(s^0) \qquad \psi_r(0) = 0.9\;\psi_r^0(s^0) \qquad s(0) = s^0 \tag{29}$$

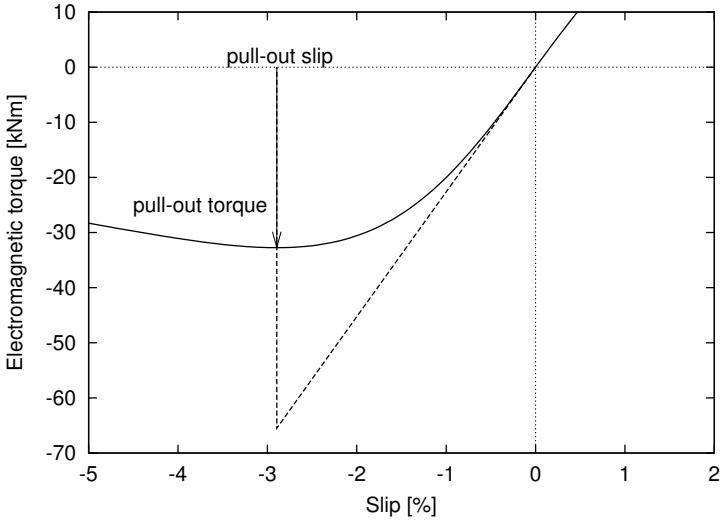

Figure 3. Steady electromagnetic torque as function of slip for a 2 MW induction machine in the generator region. The pull-out slip is 2.90 % and the pull-out torque is 32.75 kNm computed by equation (27)*. The approximate relation between slope at zero slip with these pull-out values given by* (28) *is indicated by the dashed lines.*

which together with the governing equations (14) and (22) form two initial value problems. The complex integration constant c_1 of the fast components in the transient response given by (24) is determined by the difference between the steady state stator flux and the initial stator flux ($c_1 = \psi_s^0 - \psi_s(0) = 0.1\ \psi_s^0(s^0)$).

A steady slip of -0.8 % is chosen for the simulations, which corresponds to a mechanical torque of approximately 16.6 kNm. Figure 4 shows time series with a length of 1 s of the rotor and stator fluxes, slip, and electromagnetic torque. All results based on the reduced model seems to capture the slow averaged variations described by the full model. Only small deviations between the perturbation solution and the full model are seen when comparing the fast transients computed using (24) added to this average response predicted by the reduced model. The decaying amplitudes of the fast transients are well described by the perturbation solution, however there seems to be phase shifts of the slow averaged variations. These phase shifts (or frequency shifts) occur at the beginning of the time series, where the fast transients are largest. This observation indicates that the shifts are caused by the earlier mentioned effect of large fast variations on the slow averaged variations.

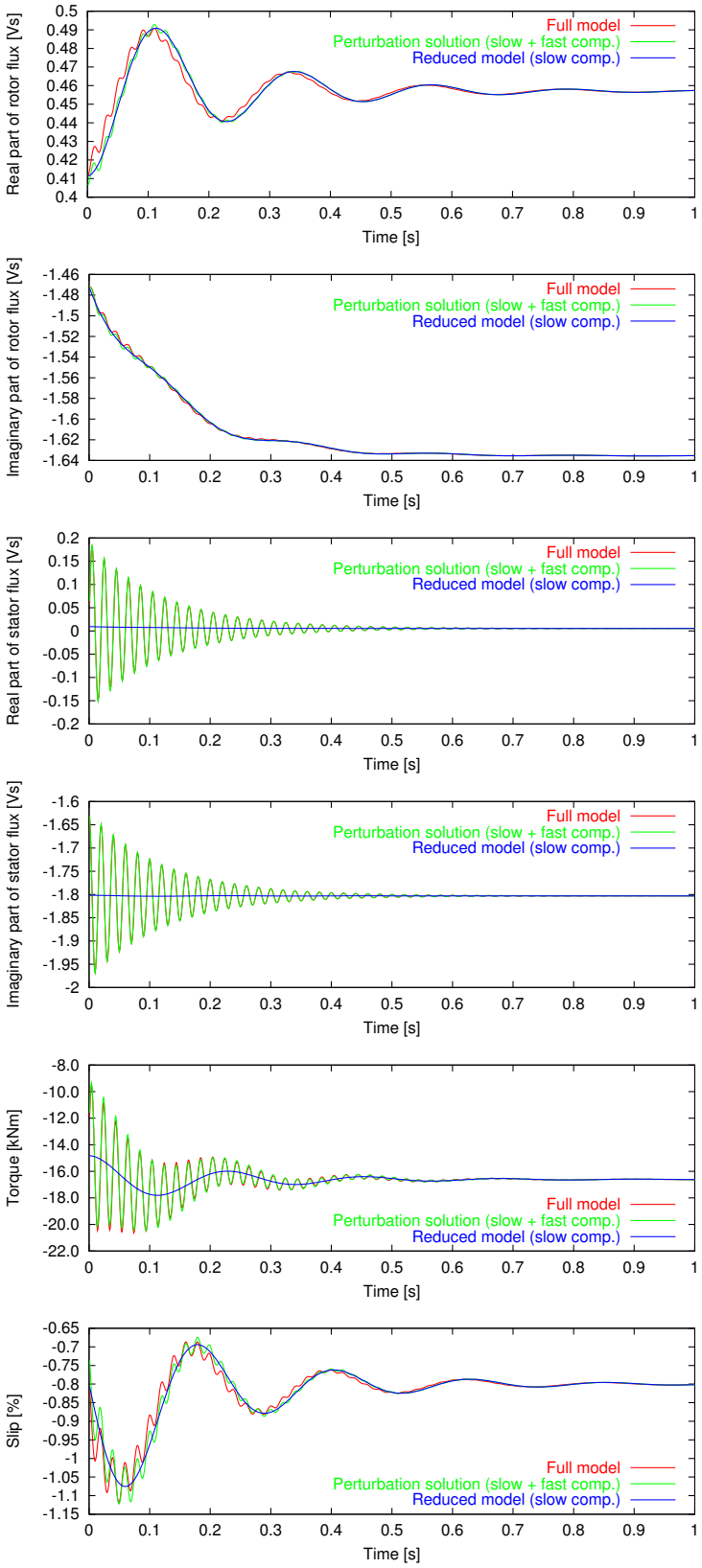

Figure 4. Time series from simulations of transients based on the full and reduced models. The fast varying overlay on the slow variations predicted by the reduced model are computed by equations (24).

Natural generator frequency

The simulations in Figure 4 shows that the slow average part of the transients has a distinct frequency of little more than four oscillations per second. Similar to a mass-spring system, this low natural frequency of the generator corresponds to the moment of inertia J being supported by the magnetic generator moment, however the equivalent spring stiffness is not directly given.

Because there is a good agreement in the simulation between the full and reduced models in the low frequency response, the reduced model is considered for the derivation of this low natural frequency of the generator. The equations of slow variations (22) are linearized by assuming small perturbations about the steady state equilibrium given by (25). The linear equation for the rotor flux is then rewritten on real form which together with the linear equation for the slip leads to a set of three first order ordinary differential equations. After reducing the terms in these equations using that the non-dimensional parameters in (13) are small, the following characteristic matrix is obtained:

$$\mathbf{A} = \begin{bmatrix} \omega_e\,\gamma_{rs} & -\omega_e\,s^0 & -\omega_e\psi^0_{r_{\mathrm{Im}}} \\ \omega_e\,s^0 & \omega_e\,\gamma_{rs} & \omega_e\psi^0_{r_{\mathrm{Re}}} \\ -\frac{3}{2}\frac{p^2\,L_m\,(\gamma_{sm}\,\psi^0_{r_{\mathrm{Re}}}-\psi^0_{s_{\mathrm{Im}}})}{J\,\omega_e\,D} & -\frac{3}{2}\frac{p^2\,L_m\,(\gamma_{sm}\,\psi^0_{r_{\mathrm{Im}}}-\psi^0_{s_{\mathrm{Re}}})}{J\,\omega_e\,D} & 0 \end{bmatrix} \tag{30}$$

where s^0 is the steady slip, and the steady fluxes are written as $\psi^0_{r_{\mathrm{Re}}} + j\psi^0_{r_{\mathrm{Im}}} = \psi^0_r$ and $\psi^0_{s_{\mathrm{Re}}} + j\psi^0_{s_{\mathrm{Im}}} = \psi^0_s$, which are given by the steady slip. This characteristic matrix has three eigenvalues, a purely real eigenvalue and two complex conjugated eigenvalues. The low frequency mode observed in the transients in Figure 4 corresponds to the latter eigenvalue pair.

It is possible to derive all three eigenvalues analytically from the characteristic equation, but the resulting expressions are large and offer little insight. A simple expression for the natural frequency has been derived by Kovacs in [8], where he assumes quasi-steady conditions for the stator, neglects the resistance over the stator ($\gamma_{sm} = 0$), and linearizes about the steady state at zero slip. Introduction of the same assumptions and derivation of the complex eigenvalues of $\mathbf{A}$, the simple expression can be rewritten as

$$\omega_{s^0=0} = \omega_e \sqrt{\frac{2T_p}{T_{initia}} - \frac{s_p^2}{4}} \tag{31}$$

where T_p and s_p are the numerical values of the pull-out torque and slip given by (27), and $T_{initia} \equiv J\,\omega_e^2/p$ is a characteristic torque due to the inertia of the generator and added mass of adjacent parts of the high speed shaft.

Figure 5 shows the natural frequency and damping in logarithmic decrement as function of the steady slip from 0 to s_p. The natural frequency decreases, whereas the damping increases, with the numerical value of the steady slip. The frequency predicted by equation (31) remains constant because it derived based on a zero slip steady state condition. From zero to pull-out slip, the frequency decreases about 20 %, while the damping is more than doubled. The results shows good agreement between the reduced model and the full model.

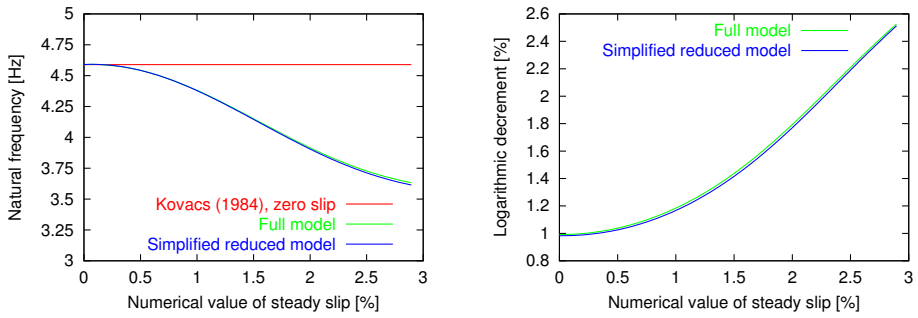

Figure 5. Natural frequency and damping of the low frequency mode of a 2 MW machine as function of the steady slip computed by eigenvalue analysis of the full and reduced models, and the equation (31) *given by Kovacs [8].*

The existence of this low frequency mode in the generator is important knowledge for the aeroelastic analyst of wind turbines. The mode may interact with the turbine structure, and it must therefore be modelled in the aeroelastic turbine codes. The reduced model has proven to sufficient to capture this low frequency response of the generator. Furthermore, designers may use the simple expression (31) to predict the natural frequency, but shall be aware that the result is very dependent on the moment of inertia J that is used for such prediction.

4 Generator characteristic

In the following the generator model (5) is considered for an asynchronous generator, which is characterized by a short-circuited rotor, i.e., the rotor voltage is zero. The static relation between generator torque and generator slip (obtained by increasing the rotor speed very slowly in (9) and (10)) is illustrated in Figure 6.

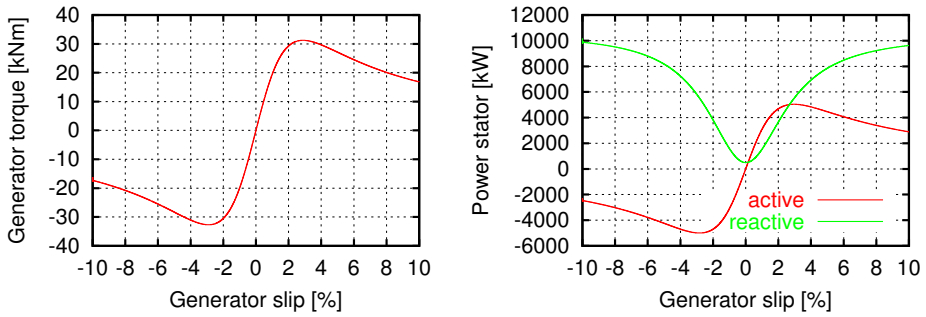

Figure 6. Characteristic of an asynchronous generator. Left: Relation between torque and slip. Right: relation between active/reactive power and slip.

The static torque characteristic in Figure 6 is normally used to confirm the liability of simple linear static generator models, where the torque is linearized around the synchronous speed (s=0).

An interesting question is whether the dynamic formulation of generator flux causes a noticeable change in slope or whether significant hysteresis loops will occur due to dynamic input since this will change the effective generator characteristic.

In Figures 7 and 8 two different frequency input are applied to the reduced dynamic model. The frequency input in Figure 7 of 1.5 Hz corresponds to the typical aerodynamic input frequency of main shaft torsion of a 500 kW turbine with a rated speed of 0.5 Hz. This frequency is higher than for a 2 MW turbine but illustrates the generator behavior at low vibration frequency. For a 2 MW turbine the frequency is app. 0.8 Hz. For such a frequency the loops are more narrow (and fits better with the static solution) than illustrated in Figure 7. The frequency input of 10 Hz in Figure 8 is included in the report to illustrate the behavior of the generator regarding higher frequencies in the drive train. It can be seen that not only are the loops in Figure 7 rather open, but at the high frequency of 10 Hz a change in effective slope occurs. This means that the characteristic of the generator is much different at high frequencies than assumed from a static point of view which causes a lower damping contribution from the generator to higher order vibration modes of the drive train.

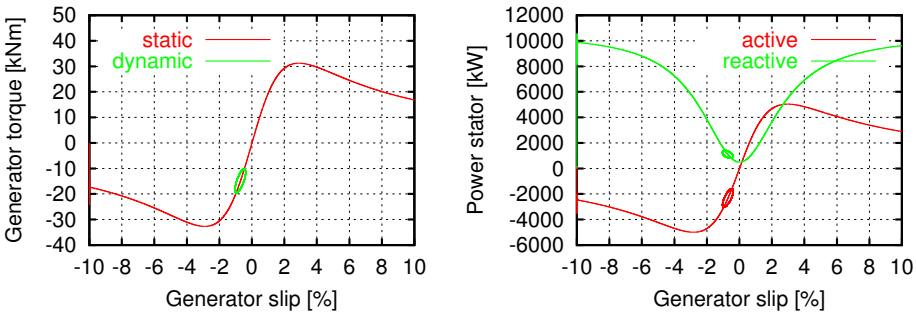

Figure 7. Dynamic variation in rotor speed of 1.5 Hz. Left: Generator torque static and dynamic. Right: Active and reactive stator power static and dynamic.

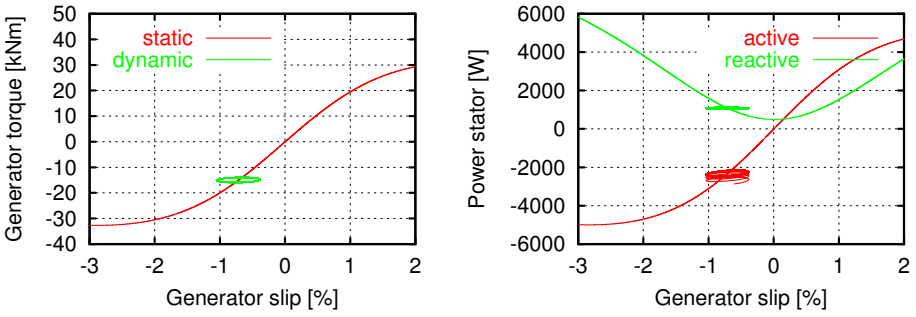

Figure 8. Dynamic variation in rotor speed of 10 Hz. Left: Generator torque static and dynamic. Right: Active and reactive stator power static and dynamic.

5 Implementation in the aeroelastic code HAWC

The new generator model is implemented in the aeroelastic code HAWC. In the following a short description of this code is given together with a short implementation of how the new model is implemented.

5.1 Short description of HAWC

HAWC [12] is a computer program with the purpose of predicting load response for a horizontal axis two and three bladed wind turbines in the time domain. The program consists of several sub-packages each dealing with a specific part of the turbine and the surroundings.

The core of the program is the structural model, which is a finite element model based on Timoshenko beam elements. The turbine is divided into three substructures: Tower, nacelle and rotor blades. Each substructure has its own coordinate system allowing for large rotation of the substructures. There are six degrees of freedom (DOFs) for each element node, i.e., for at typical wind turbine the total number of DOFs are approximately 250.

The aerodynamic model is based on a modified Blade Element Momentum (BEM) model. This model have through the years of development evolved from a static frozen wake method to a dynamic wake formulation including corrections for yawed flow. The local aerodynamic load is calculated at the blade sections using 2D lift, drag and moment profile coefficients. Unsteady aerodynamic effects are modelled by a Beddoes-Leishman type dynamic stall model.

The wind field turbulence model used for load simulations is the Mann model [13]. This model is a full 3D turbulence field with correlation between the turbulence in the three directions. The turbulence field is a vector field in space, a so-called frozen snapshot of the turbulent eddies in the wind. This turbulence is transported through the wind turbine rotor with the speed of the mean wind speed.

The HAWC model is equipped with interface for control systems through a Dynamic Link Library (DLL) format [14]. This interface enables control of the turbine pitch angles and generator torque from a control program outside the HAWC core.

The standard generator model used primarily for fixed speed stall regulated turbines is a linear slip model. This model have only 3 input parameters (nominal slip, rated power, rated generator speed). Additionally the generator efficiency must be supplied. The model is simple, but very robust and for many applications sufficient regarding aeroelastic calculations.

Some extra features regarding offshore foundations and wave interactions are also sub-packages in the program, but not used for simulations related to this report.

5.2 Practical implementation

The new generator model is implemented as an alternative to the existing linear static generator model. To enable the implementation of the new generator model, the torque from the generator is added to the structural model of the drive train as an external moment. Input to the generator model is apart from the information used for initialization simplified to only include the rotational speed of the generator and the voltage of stator and rotor.

Initialization

In the generator initialization the constant variables (L_m, L_{rr}, L_{ss}, D, ω_e) in the model is calculated based on the input variables for the generator (R_s, X_s, R_r, X_r, X_m, R_m, f_{net}, p). Usually these parameters can be obtained from the generator data sheet. In the initialization a logical switch i implemented. This determines whether a full dynamic solution, a reduced dynamic solution or a static solution of the generator flux is requested.

Calculation of torque during simulation

The torque is computed in each time step (and iteration) in the aeroelastic simulation. The input values are values of the stator and rotor voltage and the state variable of generator speed and acceleration ($u_s, u_r, \omega_r, \dot{\omega}_r$). The output is generator torque for the next time step. During the aeroelastic simulation, the nonlinear structural and aerodynamic equations are solved iteratively to obtain balance.

The magnetic flux of the rotor is calculated from (9) using a Runge-Kutta method written for complex variables. The flux of the stator is calculated on basis of (5), (10) or a static solution of (5) depending of the logical switch stated above. The torque is calculated on basis of (8).

Calculation of power and current during simulation

Based on the results of fluxes calculated above, the current of the rotor and stator is calculated on basis of (4) and the electrical power by (6).

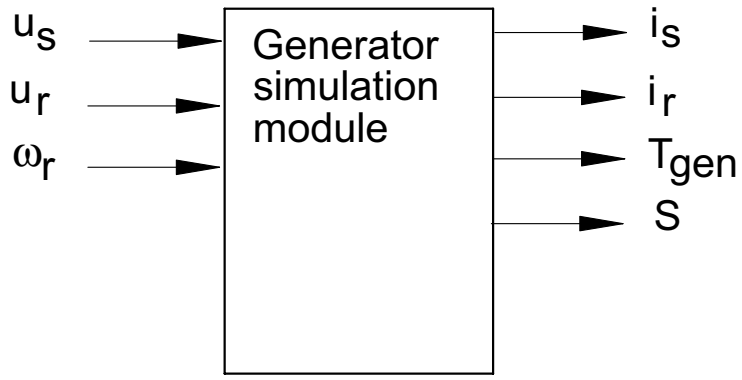

Figure 9. Illustration of in- and output from the generator module during simulations. Input is voltage of stator and rotor and the rotational speed of the rotor. Output is current of stator and rotor, generator torque and apparent power S.

6 Test cases

In the following a wind turbine model with the new reduced dynamic generator model has been simulated in a few load situations. Previously in Section 2 a cut-in situation has been simulated with both full dynamic model and reduced dynamic model with focus on the transients. In this section more common production load cases at 6 and 20 m/s with turbulence are simulated as well as a wind step situation with homogeneous wind.

6.1 Turbine properties

The test turbine is a fixed pitch, constant speed, stall-regulated turbine. The main turbine characteristics are listed in Table 2, and the specific generator data are listed in Table 3

Turbine data

Component	Parameter	Value
Rotor	Power regulation	Fixed pitch stall
	Number of blades	3
	Rotor diameter	76 m
	Hub height	60.0 m
	Rotational speed (rated)	16.9 rpm
	Rated power	2.0 MW
	Tilt angle	6°
	Cone angle	0°
	Direction of rotation	clockwise seen from the wind
	Cut-in wind speed	5 m/s
	Cut-out wind speed	25 m/s
Blade	Type	
	Material	Glass fiber w. polyester
	Length	36.8 m
	Max. chord at $r_{blade} = 3m$	2.7 m
	Twist	15.5°
Drive train	Type	Gearbox acting as 2^{nd} main bearing
	Generator	Asynchronous
	poles	2 pairs
	Gear ratio	1:88.88
Tower	Type	Tapered, tubular - steel
	Height	58.0 m
	Diameter at top	2.3 m
	Diameter at bottom	4.0 m
Mass	Blade	1700 kg
	Rotor incl. hub	54000 kg
	Nacelle, without hub or rotor	75000 kg

Table 2. Main parameters of the 2 MW turbine.

Parameter	Value	
Three phase asynchronous generator with wound rotor		
Building size	2	MW
Number of poles	4	
Moment of inertia	65	kgm^2
-Shortcircuited rotor		
Rated frequency	50	Hz
Starting torque	10	kNm
Break down torque		
-Generator	39	kNm
-Motor	37	kNm
-Equivalent circuit diagram (delta connection) **-Values at stator side** **-Values transformed to an equivalent star connection**		
Stator resistance R_s	1.164	mΩ
Stator leakage reactance X_s	22.0	mΩ
Magnetizing reactance X_m	0.940964	Ω
Rotor leakage reactance X_r	23.7	mΩ
Rotor resistance R_r	1.309	mΩ
Voltage U	398	V
Frequency f_{net}	50	Hz

Table 3. Generator data

Mode shape	Frequency [Hz]	Damping [%]
1^{st} tower transverse	0.39 Hz	2.9
1^{st} tower longitudinal	0.40 Hz	3.0
1^{st} rotor torsion	0.62 Hz	2.4
1^{st} asym. rotor flap/yaw	0.87 Hz	2.7
1^{st} asym. rotor flap/tilt	0.94 Hz	2.8
1^{st} sym. rotor flap	1.07 Hz	3.3
1^{st} rotor edge 1	1.72 Hz	4.0
1^{st} rotor edge 2	1.78 Hz	4.2
2^{nd} asym. rotor flap/yaw	2.05 Hz	6.3
2^{nd} asym. rotor flap/tilt	2.20 Hz	6.5
2^{nd} sym. flap	2.58 Hz	7.79
3^{rd} asym. rotor flap/tilt	3.87 Hz	14.0
3^{rd} asym. rotor flap/yaw + 1^{st} tower yaw	3.97 Hz	13.2
2^{nd} rotor edge	4.08 Hz	9.8
3^{rd} asym. rotor flap/yaw + 2^{nd} tower bending	4.43 Hz	16.7

Table 4. Calculated global mode shape frequencies of the turbine at stand-still.

Turbine eigenfrequencies and modal shape

The natural frequencies of the turbine have been calculated with the code HAWC-modal. The mode shapes at stand-still (with a clamped mechanical brake) are illustrated in Figure 10 together with the description of mode shapes in Table 4.

Due to gyroscopic effects when the turbine operates, the mode shapes and frequencies change. These frequency changes are also calculated with *HAWCModal* [15] and are plotted as a campbell diagram in Figure 11.

An important structural frequency not obtained from the HAWCModal calculation is the rotational mode of the drive train with a free generator. In this mode shape, the rotor is vibrating in counter-phase with the rotor of the generator (through the gearbox). The corresponding natural frequency can be approximated by

$$f_{free-free} = \frac{1}{2\pi}\sqrt{\frac{K_{shaft}}{\left(\frac{1}{I_{rotor}} + \frac{1}{I_{gen}i_{gear}^2}\right)^{-1}}} \tag{32}$$

For the turbine with data listed above, this frequency is 1.36 Hz with $K_{shaft} = 7.55{\cdot}10^7$ Nm/rad, $I_{rotor} = 7.58{\cdot}10^6$ kgm^2, I_{gen}=150 kgm^2, gear ratio i_{gear}=88.88).

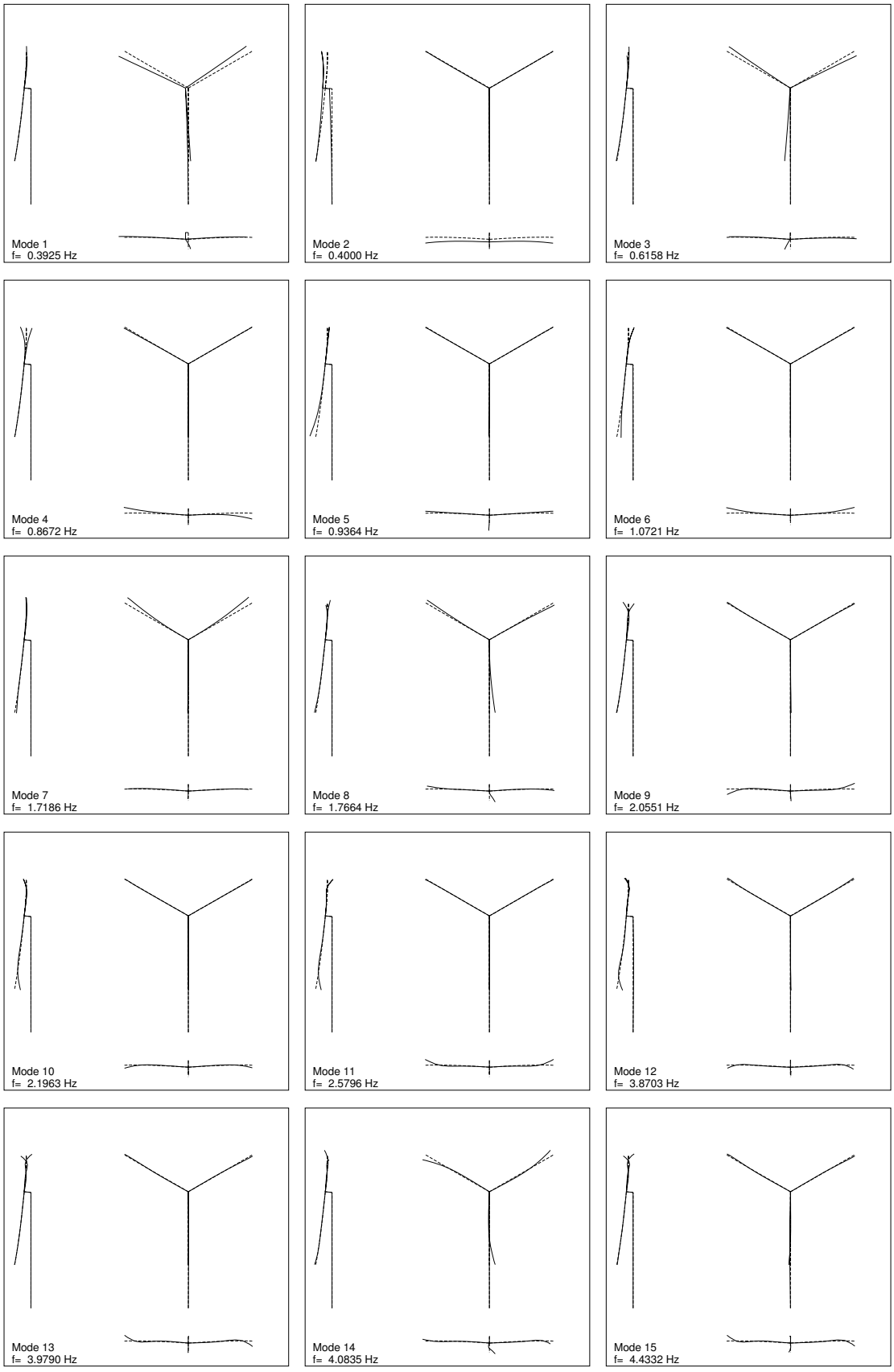

Figure 10. Mode shapes of the 2MW wind turbine at stand still. Negative (full line) and undeformed (dashed) are illustrated. See list of frequencies in Table 4.

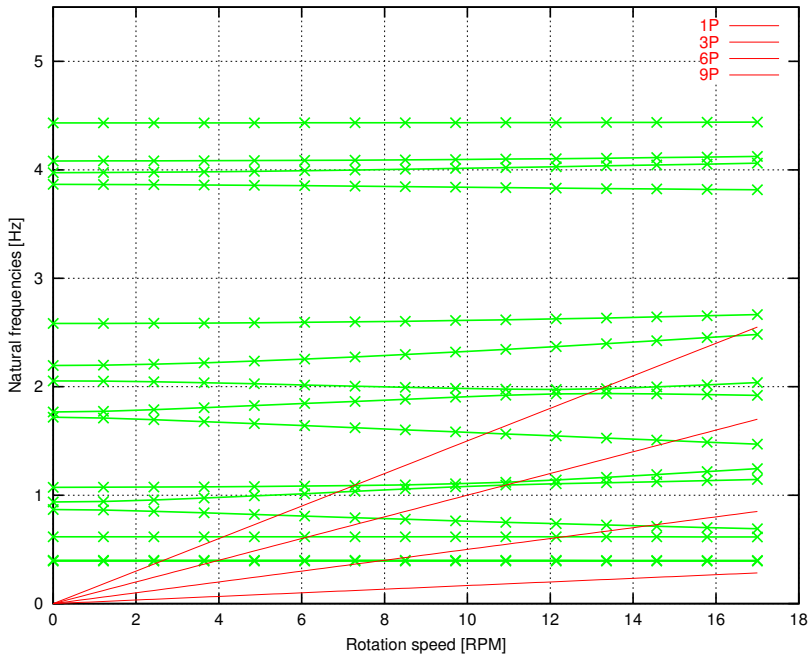

Figure 11. Campbell diagram of the turbine natural frequencies as function of rotational speed. See list of frequencies in Table 4.

Frequency coincidence at 4.5 Hz

Figure 11 shows that the turbine has a natural frequency at 4.4 Hz. In the corresponding mode shape, the turbine vibrates in a combination of the 3^{nd} flapwise bending mode of the blades and the 2^{nd} lateral bending mode of the tower. This particular natural turbine frequency is close to the natural frequency of the generator (see Section 3.3). The turbine mode may therefore couple during operation with the generator mode. This coupling may explain the large tower moment amplitudes at a wind speed of 20 m/s seen in Figure 12.

The turbine mode at 4.4 Hz is primarily a rotor mode. If the tower is modelled infinitely stiff, the turbine still has a natural frequency close to 4.5 Hz, and the corresponding mode shape is similar to the original shape, except for vanishing tower amplitudes. The coupling between this rotor mode and generator mode still exist, although the tower loads for this configuration does not increase during the simulation as in Figure 12, but remain at a constant level.

The critical coupling between a turbine mode and the generator mode is completely removed, if there is no natural turbine frequencies close to 4.5 Hz. This situation is tested by modelling the blades and tower as infinitely stiff. The result is shown in Figure 13, where there are no significant vibrations at 4.5 Hz. The coupling between a turbine and generator mode is also removed if the generator is modelled by a purely quasi-steady model, because the generator mode in this case vanish.

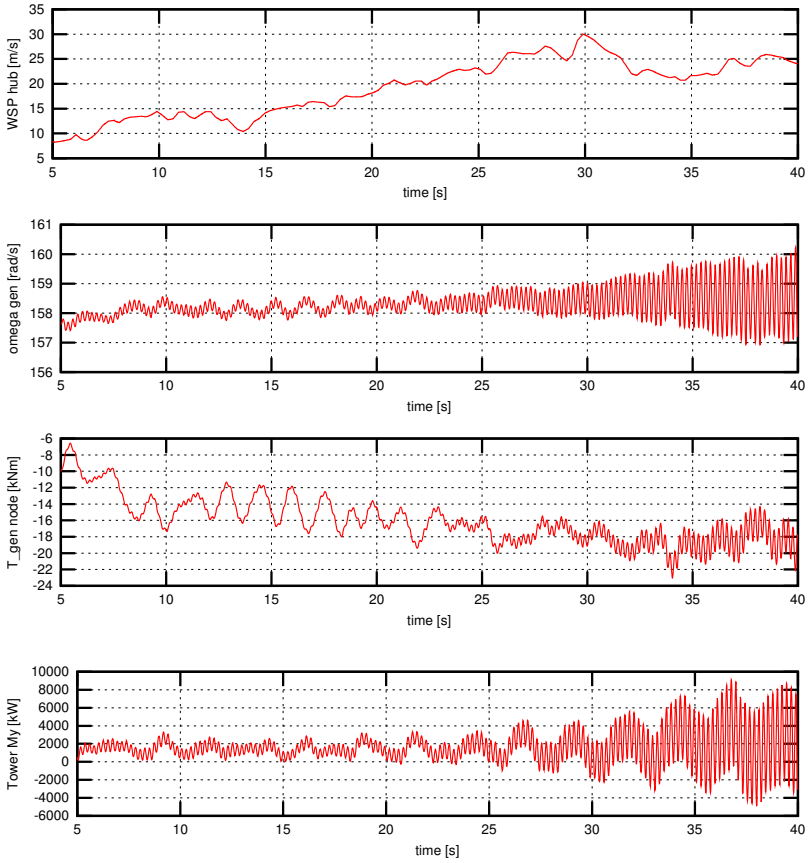

Figure 12. Simulation at 20 m/s with the reduced dynamic generator model. There is a coupling between a global turbine vibration mode and a generator eigenfrequency resulting in large vibrations at 4.5 Hz, especially for the tower. From top: Wind speed at hub [m/s], rotational speed generator [rad/s], mechanical generator torque [kNm], tower bottom lateral bending moment [kNm]

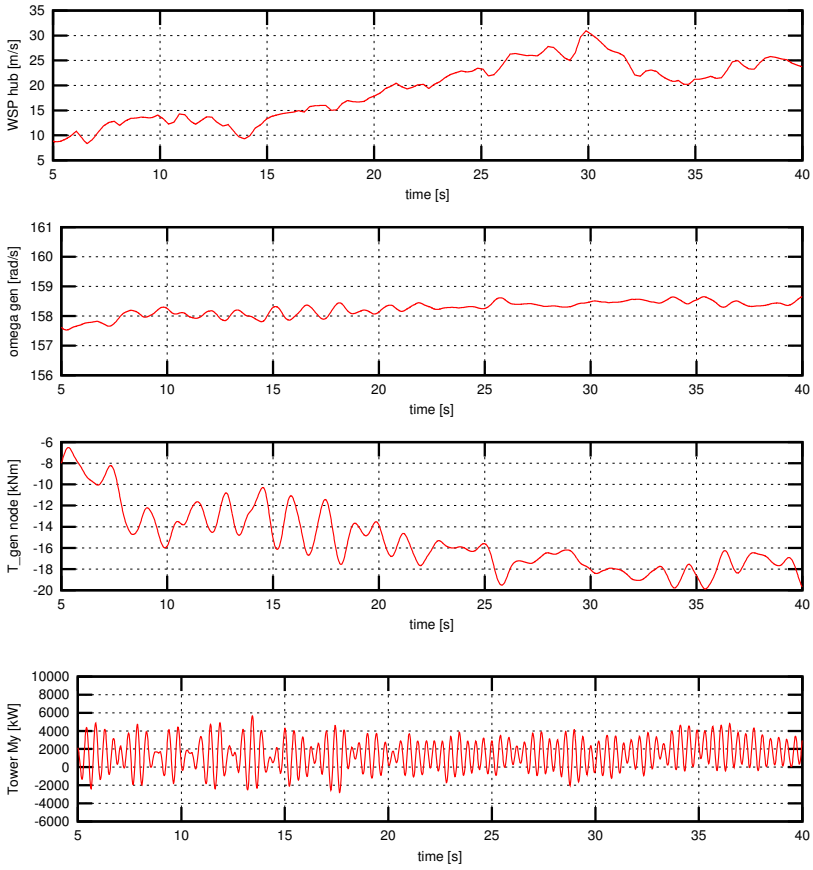

Figure 13. Simulation at 20 m/s with the reduced dynamic generator model. The blades and the tower is assumed to be stiff. From top: Wind speed at hub [m/s], rotational speed generator [rad/s], mechanical generator torque [kNm], tower bottom lateral bending moment [kNm]

6.2 Homogeneous flow at 6 m/s with wind step to 10 m/s

The first test case is to examine the response when a step input in wind speed occurs. The transient response of the generator (and the dynamics of the turbine) can be observed in Figure 14.

The difference in this special load case between the dynamic generator model and a traditional static slip model is illustrated in Figure 15.

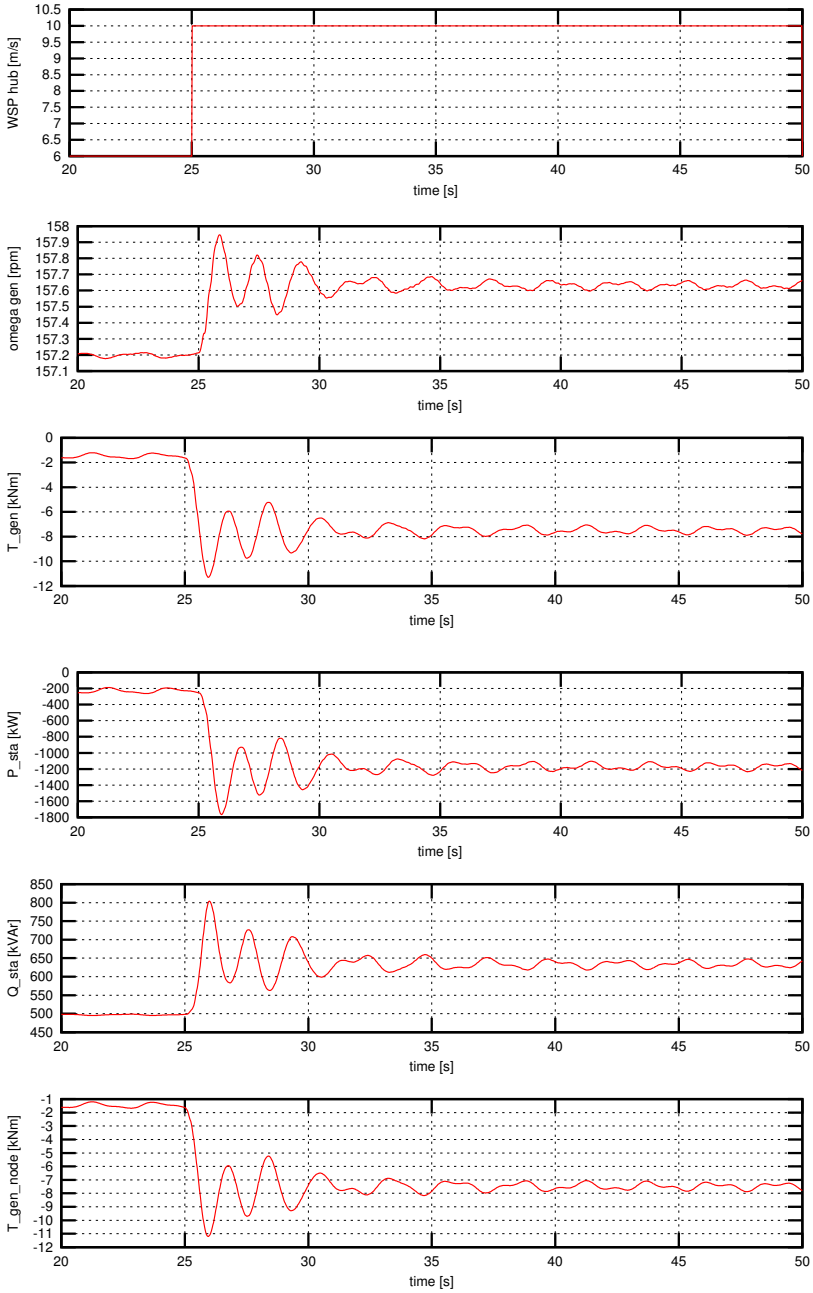

Figure 14. Step in wind speed from 6 m/s to 10 m/s. From top: Wind speed at hub [m/s], rotational speed generator [rpm], generator torque [kNm], active power stator P [kW], reative power stator Q [kVAr], shaft torque [kNm]

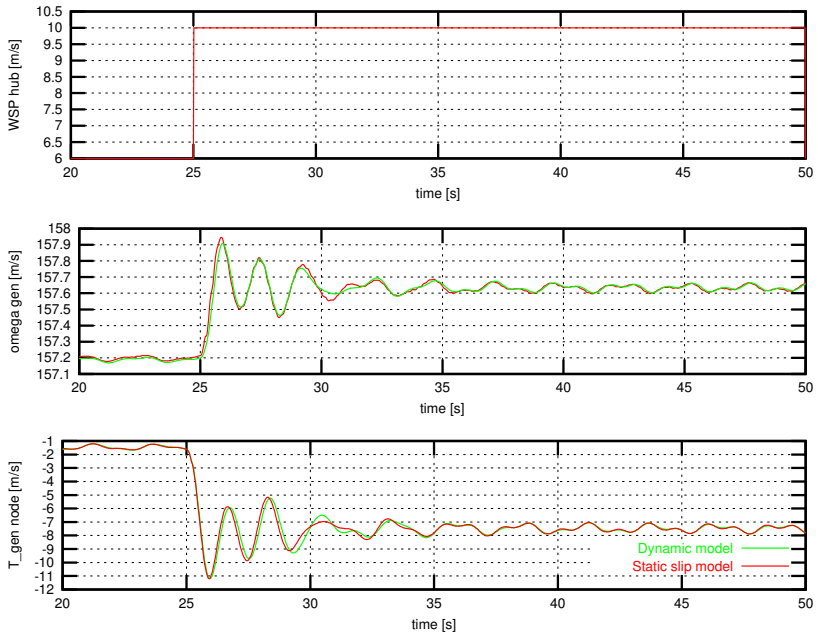

Figure 15. Comparison of response between the dynamic generator model and a traditional static slip model.

To illustrate the dynamics of the generator the generator torque as function of rotational speed is plotted in Figure 16. From this figure it can be seen that the loops characteristics in Section 4 also occurs during time simulation of the entire wind turbine.

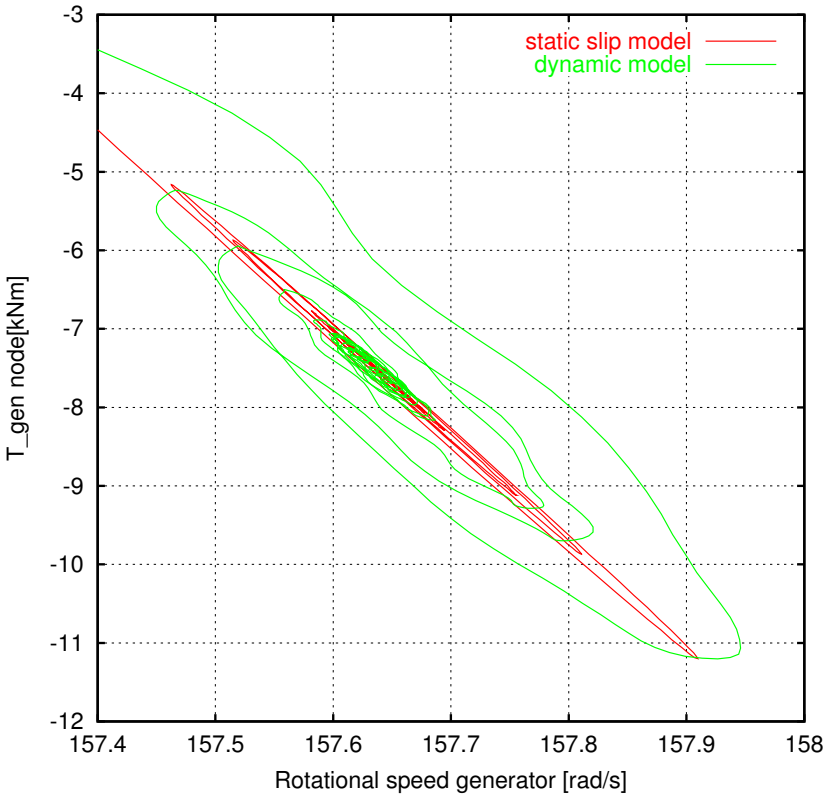

Figure 16. Illustration of difference in dynamic loops of the dynamic generator model and a static slip model during step in wind speed from 6 m/s to 10 m/s.

6.3 Turbulent flow 6m/s

A time simulation with a mean wind of 6 m/s and a turbulence intensity of 10 % has been performed to illustrate the generator behaviour at low wind speed. The result of 100 s long time simulation can be seen in Figure 17.

To evaluate the difference in dynamic response compared to a traditionally used static slip model two sets calculations have been performed. The frequency power spectra of selected sensors can be seen in Figure 18. From these spectra it can be seen that a frequency of approximately 4.5 Hz appears when the dynamic model is used. This frequency is described in Section 3.3 and 6.1.

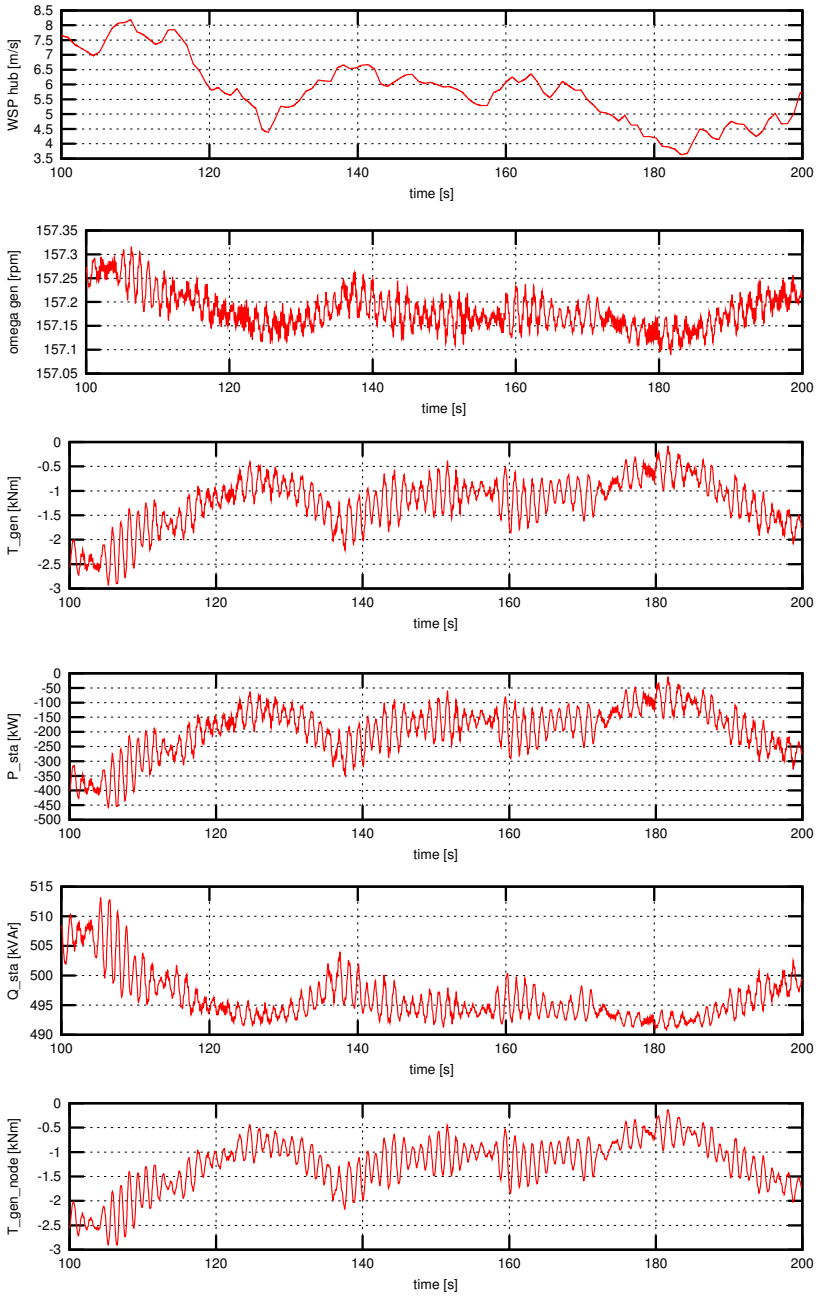

Figure 17. Simulation at 6 m/s with turbulence intensity of 10 %. From top: Wind speed at hub [m/s], rotational speed generator [rad/s], generator torque [Nm], active power stator [kW], reactive power stator [kVAr], active current stator [Amp], reactive current stator [Amp].

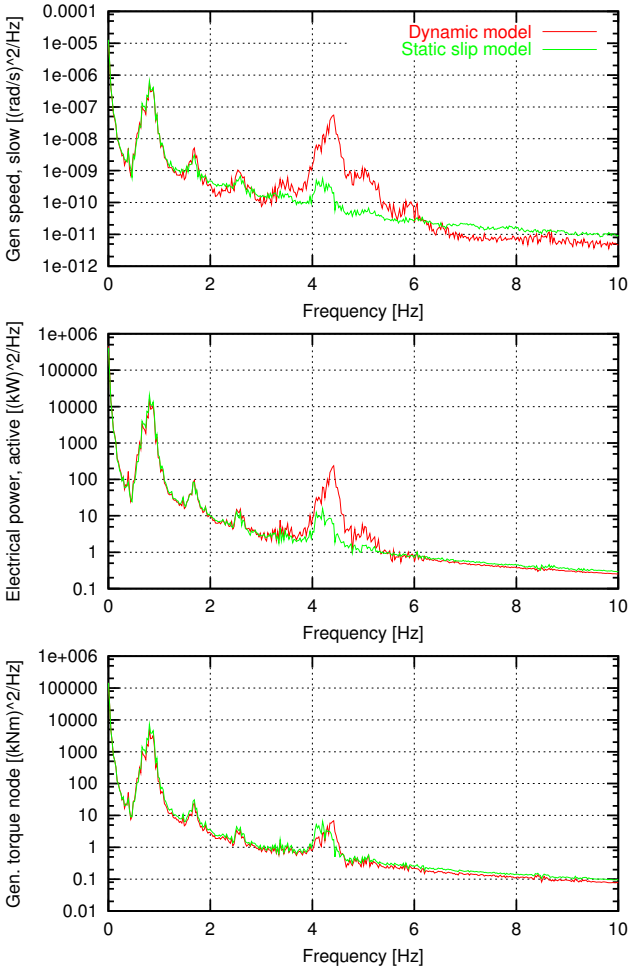

Figure 18. Power spectra. From top: Rotational speed of generator (transformed to low speed shaft), electrical power stator, generator torque including inertia effects.

6.4 Turbulent flow 20 m/s

A time simulation at 20 m/s with a turbulence intensity of 10 % has been performed to illustrate the generator behavior at high wind speed. The result of 100 s time simulation can be seen in Figure 19.

To evaluate the difference in dynamic response compared to a traditionally used static slip model two sets calculations have been performed. The frequency power spectra of selected sensors can be seen in Figure 20. From these spectra it can be seen that also for this simulation a frequency of approximately 4.5 Hz appears when the dynamic model is used. This frequency is even more visible in this simulation than the 6 m/s simulation. The frequency is described in Section 3.3 and 6.1.

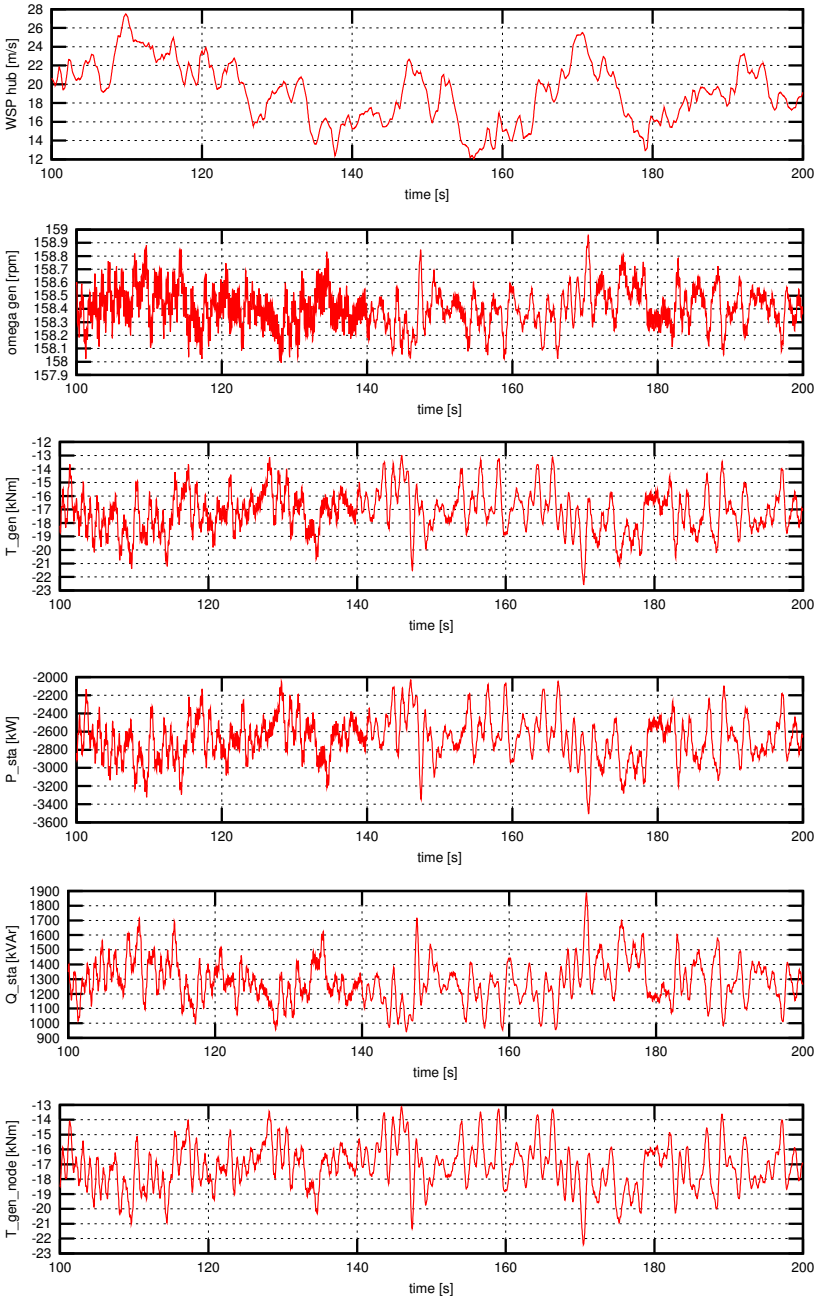

Figure 19. Simulation at 20m/s with turbulence intensity of 10%. From top: Wind speed at hub [m/s], rotational speed generator [rad/s], generator torque [Nm], active power stator [kW], reative power stator [kVAr], active current stator [Amp], reactive current stator [Amp].

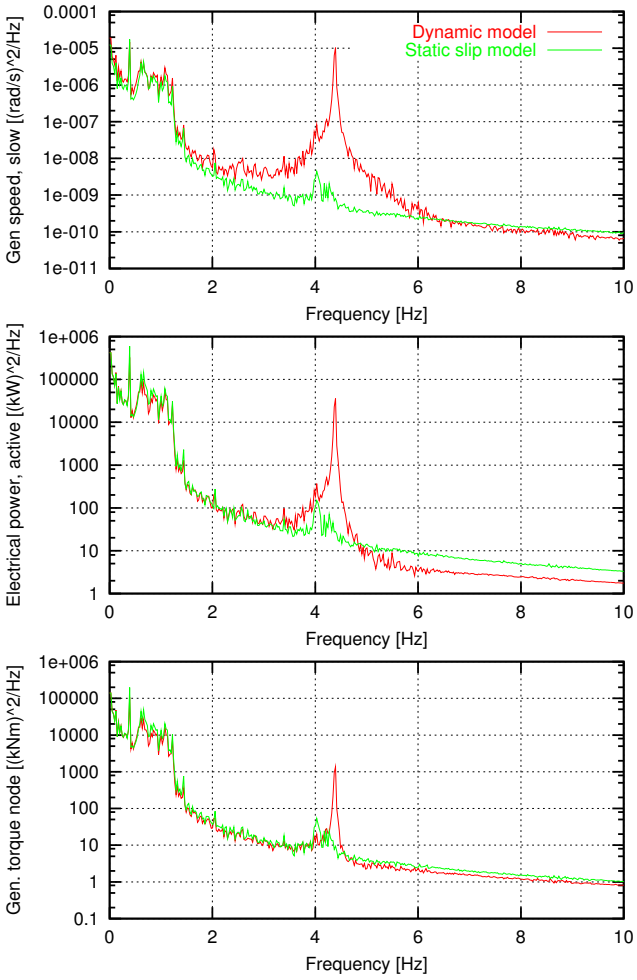

Figure 20. Power spectra. From top: Rotational speed of generator (transformed to low speed shaft), electrical power stator, generator torque including inertia effects.

7 Results and conclusions

A new generator model is implemented in the aeroelastic wind turbine code HAWC. The generator model can be used as a replacement of the existing linear static model, but can also be used to simulated the response of a doubly-fed induction generator. A reduced order model neglecting the stator flux dynamic is derived from the original full dynamic equations for the generator in a way that enables numerically solution at sample frequencies down to 40–50 Hz, corresponding to a range normally used in aeroelastic wind turbine simulations. Using a perturbation method this simplification is shown to be acceptable together with comparisons between the full dynamic model and the reduced model. The full model, needing a 1000 Hz sample frequency, is also implemented, and numerical results of both models are compared. This comparison shows that the reduction has a very little influence on the mechanical loads.

An interesting result of the simulations is the dynamic effects in the generator response. The dynamic loops in a torque–slip diagram seem to be more open than initially assumed, though dependent of the frequency. Furthermore, also the effective slope of these loops are frequency dependent. At high frequencies the torque–slip characteristic becomes nearly flat, which results in lower damping of higher order vibration modes of the drive train.

A basic natural frequency of the induction generator is derived from an eigenvalue problem formulated for the fluxes coupled to the generator slip. This frequency corresponds to a generator mode, where the inertia of the generator (including added mass of the high speed shaft and brake) is supported by magnetic forces similar to a simple mass–spring system. For a short-circuited generator, it is shown that this natural frequency decreases slightly as the numerical value of the slip increases, whereas the damping of this generator mode is increased with the slip. For the 2 MW generator investigated the frequency reduction is app. 8 % from zero slip to 1 % slip.

Coupling between the turbine modes and the generator mode can result in an instable vibration mode; this coupling cannot be detected unless a dynamic generator model is applied. Simulations for a 2 MW turbine shows a coupling between a turbine mode (involving the 3^{nd} flapwise blade mode and the 2^{nd} lateral tower bending mode) and a generator mode at a frequency of 4.4 Hz, which results in large amplitude vibrations with very high loads, especially for the tower. The instability is not seen in simulations with a linar static generator model, or if the modelled blade eigenfrequencies are changed.

A direct cut-in situation has been investigated. The situation results in transients with a frequency of the grid (50 Hz in this case) which is mainly seen on the electrical variables of the generator and the generator electro-mechanical torque. On the structural side of the generator these high frequency transients are heavily damped and they can therefore from a structural point of view be neglected.

References

[1] P. C. Krause, O. Wasynczuk, and S. D. Sudhoff. *Analysis of Electric Machinery*. IEE Press, 1995. ISBN 0-7803-1101-9.

[2] E. Drenam, S. Ahmed-Zaid, and P. W. Sauer. Invariant manifolds and start-up dynamics of induction machines. *Power Symposium, 1989, Proceedings of the Twenty-First Annual North-American*, pages 129–138, 1989.

[3] S. Ahmed-Zaid and M. Taleb. Structural modelling of small and large induction machines using integral manifolds. *IEEE Trans. on Energy Conversion*, 6(3):529–535, 1991.

[4] G. G. Richards and O. T. Tan. Simplifyied models for induction machines transients under balanced and unbalaced conditions. *IEEE Trans. on Industry Applications*, 3(1):15–21, 1981.

[5] G. G. Richards. Reduced order model for single and double cage induction motors during start-up. *IEEE Trans. on Energy Conversion*, 3(2):335–341, 1988.

[6] P. W. Sauer, S. Ahmed-Zaid, and P. V. Kokotovic. An integrated manifold approach to reduced order dynamic. *IEEE Trans. on Power Systems*, 3(1):17–23, 1988.

[7] P. V. Kokotovic and P. W. Sauer. Integral manifold as a tool for reduced-order modelling of non-linear systems: a synchronous machine case study. *IEEE Trans. on Circuits and Systems*, 36(3):403–410, 1989.

[8] P. K. Kovacs. *Transient Phenomena in Electrical Machines*. Elsevier Science Publishers B. V., 1984.

[9] T. Thiringer. Measurement and Modelling of Low-Frequency Disturbances in Induction Machines. Technical Report 297, Department of Electric Power Engineering, Chalmers University of Technology, Sweden, October 1996.

[10] I. I. Blekhman. *Vibrational Mechanics – Nonlinear Dynamic Effects, General Approach, Applications*. World Scientific, 1999.

[11] J. J. Thomsen. Theories and experiments on the stiffening effect of high-frequency excitation for continuous elastic systems. *Journal of Sound and Vibration*, 260:117–139, 2003.

[12] J. T. Petersen. The Aeroelastic Code HawC - Model and Comparisons. In *28^{th} IEA Experts Meeting: 'State of the Art of Aeroelastic Codes'*. DTU, Lyngby, 1996.

[13] J. Mann. Wind Field Simulation. *Prob. Engng. Mech., Elsevier Science*, vol. 13(no. 4):pp. 269–283, 1998.

[14] T. J. Larsen. Description of the DLL Regulation Interface in HAWC. Technical Report Risø-R-1290(en), Risoe, National Laboratory, September 2001.

[15] M. H. Hansen and A. M. Hansen. HAWCModal Wind Turbine Modal Analysis Tool – User's Guide. Technical Report Risø-I-1855(EN), Risoe, National Laboratory, 2001.

Bibliographic Data Sheet **Risø-R-1395(EN)**

Title and author(s)

Generator Dynamics in Aeroelastic Analysis and Simulations

Torben J. Larsen, Morten Hartvig Hansen, Florin Iov

ISBN	ISSN
87-550-3188-9; 87-550-3189-7 (internet)	0106-2840

Dept. or group	Date
Wind Energy Department	May 2003

Groups own reg. number(s)	Project/contract No.
1115025-1	EFP-1363/01-0013
1110036-0	ENS-1363/02-0011
1110038-0	NNE5-CT-2002-00627

Pages	Tables	Illustrations	References
45	4	19	7

Abstract (Max. 2000 char.)

This report contains a description of a dynamic model for a doubly-fed induction generator. The model has physical input parameters (voltage, resistance, reactance etc.) and can be used to calculate rotor and stator currents, hence active and reactive power.

A perturbation method has been used to reduce the original generator model equations to a set of equations which can be solved with the same time steps as a typical aeroelastic code. The method is used to separate the fast transients of the model from the slow variations and deduce a reduced order expression for the slow part.

Dynamic effects of the first order terms in the model as well as the influence on drive train eigenfrequencies and damping has been investigated. Load response during time simulation of wind turbine response have been compared to simulations with a traditional static generator model based entirely on the slip angle.

A 2 MW turbine has been modelled in the aeroelastic code HAWC. When using the new dynamic generator model there is an interesting coupling between the generator dynamics and a global turbine vibration mode at 4.5 Hz, which only occurs when a dynamic formulation of the generator equations is applied. This frequency can especially be seen in the electrical power of the generator and the rotational speed of the generator, but also as torque variations in the drive train.

Descriptors INIS/EDB

COMPUTERIZED SIMULATIONS; DYNAMIC LOADS; INDUCTION GENERATORS; MECHANICAL VIBRATIONS; PERTURBATION THEORY; WIND TURBINES

Available on request from:
Information Service Departement, Risø National Laboratory
(Afdelingen for informationsservice, Forskningscenter Risø)
P.O. Box 49, DK–4000 Roskilde, Denmark
Phone (+45) 46 77 46 77, ext. 4004/4005 · Fax (+45) 46 77 40 13
E-mail: risoe@risoe.dk